

MASARYK UNIVERSITY
FACULTY OF SCIENCE
DEPARTMENT OF PHYSICAL ELECTRONICS

**Habilitation thesis - Scientific
field: Plasma physics**

BRNO 2017

MGR. TOMÁŠ HODER, PH.D.



MASARYK UNIVERSITY
FACULTY OF SCIENCE
DEPARTMENT OF PHYSICAL ELECTRONICS



High-resolution Spectroscopy of Transient Micro-Plasmas: Discharge Mechanisms and Electric Field Determination

Habilitation thesis - Scientific field: Plasma physics

BRNO 2017

MGR. TOMÁŠ HODER, PH.D.

Abstrakt

Předložená habilitační práce se věnuje tématu fundamentálních mechanismů elektrických výbojů v tlacích blízkých atmosferickému. Shrnuje vědeckou práci autora zaměřenou na časoprostorově vysoce rozlišenou optickou emisní spektroskopii a elektrickou charakterizaci plazmatu. V práci je komentováno patnáct vědeckých článků autora. První kapitola je věnována bariérovým výbojům ve vzduchu podobných plynných směsích a jejich podrobné parametrické analýze, dále pak nestabilitám a stratifikaci plazmového filamentu ve výbojích v argonu. V druhé kapitole je popsána metoda pro určení elektrického pole s rozlišením desítek pikosekund a mikrometrů, která je aplikována na bariérové, koronové a jiskrové výboje. Věnuje se také sjednocující teorii streamerovského průrazu plynu. V poslední kapitole je popsána vylepšená metoda pro elektrickou analýzu streamerovského plazmatu.

Abstract

In the presented habilitation thesis the topic of fundamental gas discharge mechanisms in high pressure discharges is addressed. The thesis summarises the scientific contribution of the author which is focused on spatiotemporally high-resolution optical emission spectroscopy and electrical characterisation of plasmas. Fifteen articles are commented by the author. In the first chapter, the detailed parametric studies on barrier discharges in air-like mixtures and contribution to the clarification of instability-driven filament stratification in barrier discharge in argon is presented. In the second chapter, the method for high-resolution electric field determination in air-like plasmas is presented and is further applied to barrier, corona and spark discharges. It addresses the unification theory of the streamer gas breakdown mechanism, too. In the last chapter, an enhanced method of electrical characterisation of streamer driven plasmas is described.

Contents

Contents	iv
Introduction	v
Chapter 1. Advanced spectroscopy: barrier discharge mechanisms	1
1.1 The experimental techniques	2
1.2 Barrier discharges in air-like gases	3
1.3 Barrier discharge channel stratification in argon	8
Chapter 2. The electric field: a key parameter determination	11
2.1 The method	11
2.2 Trichel pulses in negative corona in air: a unification theory of the gas discharge mechanism	13
2.3 Barrier discharge on the dielectric surface	15
2.4 Barrier discharge streamer as an atmospheric lightning analog	16
2.5 The spark discharge mechanism in air	17
Chapter 3. Electrical diagnostics: an important supportive method	19
3.1 Electrical current probes and their performance	19
3.2 An equivalent circuit approach	20
References	23
Commented articles	31

Introduction

Electrical discharges in high pressure gases have characteristic time scales starting from picoseconds of electron ensemble relaxation in a given electric field and spatial dimensions of electrically highly stressed regions go down to tens of micrometers [1, 2]. Whether industrially applied coronas, sparks and barrier discharges [2, 3], or naturally occurring lightning and transient luminous events in upper atmosphere [4, 5, 6, 7], all take the form of relatively thin filaments - compared to their particular length. The whole chain of physical mechanisms of electrical gas discharges is present, making the selected discharge investigation a real challenge to experimental as well as theoretical plasma physicist.

Let us consider a gas filled space stressed by an electrical field. The first electrons generated by the background pre-ionisation (typically radioactivity, cosmic rays or residuals from a previous electrical gas breakdown) are accelerated and, depending on the gas type and electric field magnitude, they ionise the neutral surrounding gas and generate free charge carriers. This process is of statistical nature [8, 9], and depends also on material properties of electrodes [10] and their mutual spacing (if in laboratory). In barrier discharges, this process can take several microseconds until the threshold charge amount is generated and fast gas breakdown is initiated. The classical theory of John S. Townsend [11] is required in order to describe this pre-breakdown phase of the discharge. The optical emission of such a discharge-phase is typically very low and advanced sensitive techniques are necessary to enable the detection on a selected microsecond scale.

As soon as the critical free charge amount is accumulated, a fast ionising wave bridges the inter-electrode gap. The charge amount threshold is described by the electron multiplication parameter of the Raether-Meek criterion. This critical amount can be reached in one strong electron avalanche or by accumulating several sub-critical ones [9]. The breakdown via such a fast ionising wave is under given conditions named as the streamer mechanism. The streamer theory was developed independently by Walter Rogowski and Heinz Raether, in Germany, and Arthur F. Kip and Leonard B. Loeb, in USA, [12, 13, 14, 15] as a direct reaction to inconsistencies in Townsend's approach applied to the atmospheric pressure air sparks [16]. A streamer in close-atmospheric pressure gases is a contracted ionising wave that propagates into a low- or non-ionised medium exposed to a high electric field. It is characterised by a self-generated field enhancement at the head of the growing discharge channel, leaving a trail of filamentary plasma behind [17, 18]. In atmospheric pressure air, the self-generated electric field manifests itself in a form of an ultra-short electrical current pulse, typically only few units of a nanosecond.

The streamer head transforms into the cathode layer immediately after its impact onto the cathode [19, 20] or the cathode layer is created by the, in opposite direction growing, negative streamer [21]. A transient glow discharge, the third gas discharge mechanism,

takes place here. The created plasma channel is fed by a limited electrical current as it interconnects both electrodes. In barrier discharges, or transient sparks, this mechanism has only short duration. In barrier discharges, the electric field in the gap decreases rapidly due to the electric field screening by the deposited charges on the dielectric surfaces between the electrodes [22]. Consequently, the discharge channel decays due to the volume and surface recombination processes, the electrical current exponentially falls down. The whole process has few tens of nanoseconds duration in atmospheric pressure air. It was shown, that the deposited surface charges determine the further discharge behaviour [23] and can last on the surface for several hours. In transient spark discharge, the glow discharge phase is replaced by the spark mechanism and the process of discharge channel thermalisation starts. This transition takes hundreds of nanoseconds or few microseconds [24]. Due to the peaking ionisation the current and the light emission intensities are reaching their maxima during this phase. In repetitive transient spark, the power supply limits the transferred charge and stops the discharge after few microseconds.

The above described chain of discharge development can be significantly altered if inhomogeneous distributions of free charges or metastable states are present in the particular region. It can be locally enhanced density of free electrons or positive ions from the previous breakdown caught in the field-free trap and not yet drifted away, respectively. Indeed, this is the case of Trichel pulses in negative corona [25], highly-repetitive pulsed barrier discharges or kHz barrier discharges in argon. In atmospheric pressure argon barrier discharge an instability in cathode layer, caused by the overall increased energy stored in the plasma, can lead to the stratification of the discharge channel, an unwanted complication for possible applications of such plasmas. This energy amount, in form of charge or metastable states enhanced densities, can be detected only indirectly, if using optical emission spectroscopy. Moreover, one has to deal with extremely low signals, whether of light emission or of the electrical current. An advanced techniques and methods have to be applied in order to detect and resolve these phenomena.

The driving force behind all mentioned discharge mechanisms is the local electric field, whether in the charge free gap or in the streamer head. It is the electric field which accelerates electrons, enables their further multiplication, thus starting the plasma-chemistry. Consequently, new free charges are generated which rearrange the electric field distribution and so forth. Knowing its instantaneous development in all key coordinates of the discharge system gives the information necessary to understand the fundamental physics and, even better, to predict the effects of such a system on its environment. Solving the Boltzmann equation with appropriate electron and ion scattering cross sections and obtaining the electron energy distribution function for a given electric field as an input parameter [26, 27, 28] can give complete information about electron driven processes in the plasma and finally, using a kinetic model, further development of the plasma-induced chemistry can be determined [29]. Such information is crucial for optimising the performance of widely used technology of high-pressure transient plasmas in multiple industrial areas: ozone production ([30, 31, 32], barrier discharges), surface treatment ([33, 34, 35], barrier discharges, coronas), environmental uses ([36, 37], barrier discharges, coronas, sparks), plasma-assisted combustion ([38], barrier discharges, sparks), aerodynamic flow control in aircraft engineering ([39, 40], barrier discharges, sparks) or newly emerged field of plasma medicine ([41], barrier discharges, transient sparks). Moreover, the induced charge trans-

fer and plasma-chemistry in classical lightning or in upper atmospheric transient luminous events are crucial for understanding of the global electrical circuit [42], the ozone creation and destruction in the lower stratosphere [43] or the chemistry of transient luminous events at higher altitudes [44, 45].

The multi-scale nature of the physical and plasma-chemical phenomena described above truly poses an experimental challenge. The temporal and spatial scales of physical mechanisms taking place, together with the intensity of the emitted light, non-linearly change over several orders of magnitude. It requires the application of modern techniques such as streak cameras or time-correlated single photon counting enhanced spectroscopy. An advanced methodology for electrical current measurement has to be applied as well. From above mentioned reasons moreover, a sufficiently sensitive and reliable method has to be developed in order to quantify the electric field parameter in high resolution. This habilitation thesis presents the results of the author, combining above mentioned techniques and methods, and reports his contribution to the high-resolution experimental investigations of physical mechanisms in high-pressure electrical gas discharges.

It is not the intention of the author to describe the topics in all details here in the commentary part of the thesis. For more informations the reader is referred to the commented articles themselves and references therein. The author wishes you a pleasant reading.

Chapter 1

Advanced spectroscopy: barrier discharge mechanisms

Barrier discharge takes place between two electrodes where at least one of them is covered by the dielectric barrier [22]. Such a setup in which one of the electrodes is not in direct contact with the plasma prevents the discharge from sparking and the plasma maintains its non-thermal character. For barrier discharges in air, the typical temperatures are hundreds of kelvin for the electrified gas and several thousand kelvin (few units of eV) for the electrons [46, 34]. The barrier discharge in atmospheric air is typically visible as a thin violet filament of few tens of microns in diameter and bridging the inter-electrode gap. At the dielectric surface, a surface discharge spreads as a result of the impact of streamers, see schematically shown in Fig. 1.1 where the typical discharge current pulses and footprints on the electrodes are shown as well.

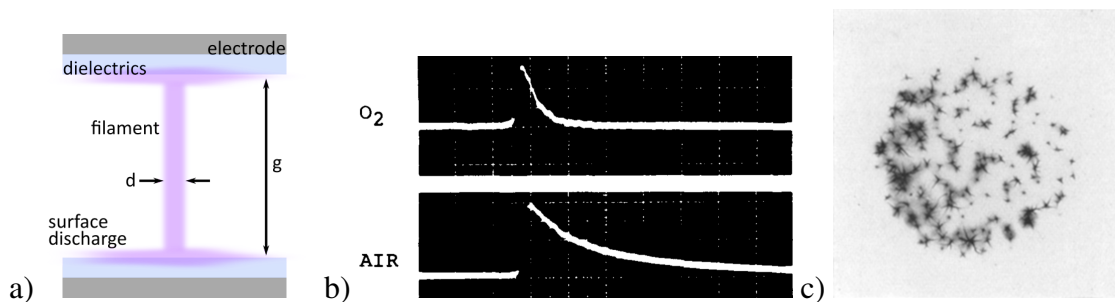


Figure 1.1: Schematic representation of single filament volume barrier discharge appearance for the naked eye a), a current pulses in oxygen and air [47] (80 mA/div and 5 ns/div) b) and Lichtenberg figures created by surface discharges of multiple filaments as recorded for the first time by Buss [48] c).

First experiments with the barrier discharges were done already by Werner Siemens [49] in 1857, who used them for generation of ozone gas. In 1932, the electrical signal was measured by Buss [48] who determined the characteristic timescale to tens of nanoseconds, took the photographical images of the discharge footprints (see in Fig. 1.1) and even estimated the electron density in the discharge channel. Later in 1943, Manley developed a method for the determination of the dissipated power in the plasma based on

the construction of charge-voltage diagrams, also called Lissajous figures. This method has a large influence even today and is still being further improved [50]¹. The far history of barrier discharge investigations and their applications is broad and its exact description is not within the scope of this work. We refer the reader to the classical texts such as the review papers of Eliasson and Kogelschatz [47, 22] or the book of Samoilovich, Gibalov and Kozlov [51].

The new era of the barrier discharge investigation starts with the first use of spatiotemporally well resolved techniques such as streak cameras [52] (see Fig. 1.2) or cross-correlation devices [53] and with the implementation of detailed computer modelling [30, 54, 20]. The mechanism of the positive streamer theoretically predicted by the models of Braun et al. [54, 20] was confirmed and the understanding further improved by spectroscopic experiments conducted by Kozlov et al. [53, 55, 56].

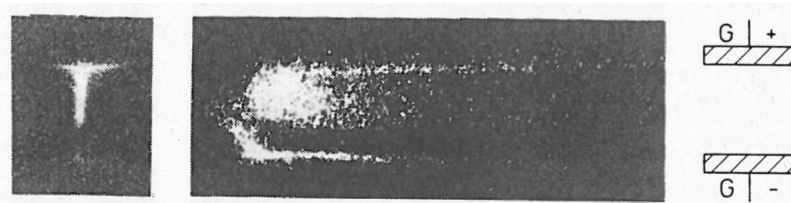


Figure 1.2: Intensified CCD (left) and streak camera (middle) recordings of the spatiotemporal distribution of the discharge channel integral luminosity in air at atmospheric pressure. The cathode directed streamer as well as the transient glow discharge structure are well visible. The inter-electrode gap is 4 mm and the time interval shown is approx. 20 ns. The picture is taken from [52].

We contributed to the understanding of barrier discharges experimentally, with support of the theoretical computer modelling. Techniques of the optical signal recording were significantly improved and mechanisms of barrier discharges in their multiple forms were clarified. In the next section, the used modern techniques of the plasma induced optical emission detection will be described. In the second section, several case studies are presented for sinusoidal and pulse driven barrier discharges in air-like gases. In the third section of this chapter, the reported studies on an instability-driven discharge channel stratification in the barrier discharge in argon are presented.

1.1 The experimental techniques

The spatial and temporal occurrence of barrier discharges has a statistical nature based on the microscopic scale of the physical phenomena taking place. As a result, barrier discharge breakdown in classical setups takes place spatiotemporally erratically. Therefore a problem of discharge detection at the right time and in the right place have to be solved. This is an important task as the signal can be very weak. Therefore, accumulative detection techniques

¹We approach this topic in more details in the last chapter where an enhanced methodology for pulsed barrier discharges is presented.

have to be used and a spatiotemporally stable and reproducible discharge operation is required.

The spatial stability of the discharge was provided by the half-spherical electrodes in our experiments with volume discharges [56, 57], by deposited parabolic copper films in the case of coplanar barrier discharge [58, 57] or using syringe needles in the case of surface barrier discharge [59]. These electrode arrangements created a confined Laplacian electric field area for the first electrons to be multiplied in. The repetitive discharge then usually followed this pre-ionised path.

The proper temporal reference to the discharge for exactly timed light detection was arranged using a master trigger signal in the case of pulsed barrier discharges [60, 61, 62]. The master trigger from the function generator synchronised the power supply and the recording interval (gate opening) of the detecting system, an intensified CCD camera or a streak camera, both usually enhanced by a far-field microscope to improve the spatial resolution. The streak camera images yield the spatiotemporal discharge development along the discharge axis during rising and falling slopes of the electrical pulse with a high temporal and spatial resolution of 50 ps and 10 μm , respectively. The spectral resolution was done using spectral filters.

In the case of sinusoidal driven barrier discharges, the stable temporal occurrence of the breakdown can not be assured and thus an advanced synchronisation technique has to be applied. We used the so called time-correlated single photon counting (TCSPC) technique, where the recorded optical signal is synchronised by the discharge itself. It is also called cross-correlation spectroscopy when the synchronisation signal is also of an optical nature. This method allows the substitution of the real-time measurement of the discharge event by a statistically averaged determination of the cross-correlation function between two optical signals, both originating from the same source. These two signals are the so called main (spatially and spectrally resolved) and the synchronising signal, see figure 1.3. The time between the synchronising signal detection and spectrally and spatially resolved single-photon count is measured. A complete measurement is supposed to correspond to the actual light emission of the single micro-discharge. The temporal resolution can go down to 10 ps in some cases. Using a straightforward optical projection onto the entrance slit of the monochromator by a UV-achromat lens, the high spatial resolution of 10 μm was achieved. As the TCSPC technique has a larger dynamic range than the streak camera used, we applied it for some selected studies also to the pulsed discharges [62].

In summary, the author and his cooperators have achieved a unique spatiotemporal resolution of up to 10 μm and 10 ps in conducted experiments. These advanced spectroscopy apparatuses then enabled, in some cases for the first time, to observe the discharge phenomena in their characteristic spatiotemporal scales and so revealed the microscopical features of the physical mechanisms taking place.

1.2 Barrier discharges in air-like gases

In this section, some selected results will be commented, which were obtained during the author's activity as postdoctoral researcher at the INP Greifswald (Leibniz Institute for Plasma Science and Technology, Greifswald, Germany, colleagues H. Höft, M. Kettlitz and R. Brandenburg) and in cooperation with the Institute of Physics, Greifswald University

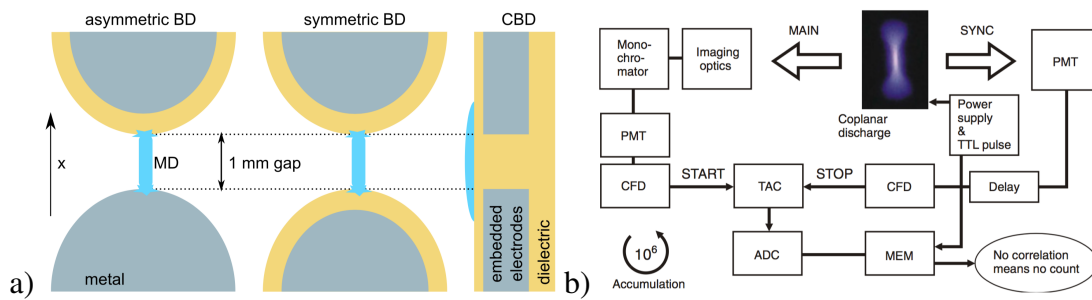


Figure 1.3: An outline of the single filament barrier discharge electrode setups a) and a scheme of the TCSPC apparatus for the case of single filament investigation (here for the coplanar barrier discharge, b). The imaging optics consists of one lens (UV, achromat); PMT—photomultiplier; CFD—constant fraction discriminator; delay—coaxial delay cable; TAC—time-to-amplitude converter; ADC—analogue-to-digital converter; MEM—memory block with up to 4096 channels. The pictures are taken from [57, 58].

in Germany (H.-E. Wagner) and Lomonosov Moscow State University in Russia (K. V. Kozlov). These experimental studies were performed on sinusoidal and pulsed barrier discharges using the above mentioned devices. The following five articles are commented:

1. **Hoder T**, Brandenburg R, Basner R, Weltmann K D, Kozlov K V and Wagner H E 2010 A comparative study of three different types of barrier discharges in air at atmospheric pressure by cross-correlation spectroscopy *Journal of Physics D: Applied Physics* **43** 124009 [57]
2. Grosch H, **Hoder T**, Weltmann K D and Brandenburg R 2010 Spatio-temporal development of microdischarges in a surface barrier discharge arrangement in air at atmospheric pressure *The European Physical Journal D* **60** 547–553 ISSN 1434-6079 [59]
3. **Hoder T**, Höft H, Kettlitz M, Weltmann K D and Brandenburg R 2012 Barrier discharges driven by sub-microsecond pulses at atmospheric pressure: Breakdown manipulation by pulse width *Physics of Plasmas* **19** 070701 [60]
4. Höft H, Kettlitz M, **Hoder T**, Weltmann K D and Brandenburg R 2013 The influence of O-2 content on the spatio-temporal development of pulsed driven dielectric barrier discharges in O-2/N-2 gas mixtures *Journal of Physics D: Applied Physics* **46** 095202 [61]
5. Höft H, Kettlitz M, Becker M M, **Hoder T**, Loffhagen D, Brandenburg R and Weltmann K D 2014 Breakdown characteristics in pulsed-driven dielectric barrier discharges: influence of the pre-breakdown phase due to volume memory effects *Journal of Physics D: Applied Physics* **47** 465206 [62]

In the first article, the comparison of the coplanar, symmetric and asymmetric volume barrier discharges in a single filament arrangement in atmospheric pressure air was

done using the TCSPC technique. The spatiotemporal development of the light emission intensity for two distinguished wavelengths were obtained. To be more precise, the intensities of the spectral bands coming from radiative electronic transitions $N_2^+(C^3\Pi_u)_{v'=0} \rightarrow N_2(B^3\Pi_g)_{v''=0}$ (band head at 391.5 nm) and $N_2(C^3\Pi_u)_{v'=0} \rightarrow N_2(B^3\Pi_g)_{v''=0}$ (band head at 337.1 nm) with 0-0 vibrational transitions were measured. These light emission spectral bands are usually denoted as the first negative (FNS) and the second positive (SPS) systems of the molecular nitrogen, respectively. The energy level thresholds of the respective radiative quantum states $N_2^+(C^3\Pi_u)_{v'=0}$ and $N_2(C^3\Pi_u)_{v'=0}$ strongly differ and therefore the electrons responsible for direct impact excitation (as it is the dominant process under given conditions) have to possess different energies, i.e. 18.7 and 11.0 eV respectively. Recording the emission intensities of the FNS and SPS, one receives hints on information about the electron energy distribution in the plasma. Applying a simple kinetic model, the local electric field strength can be determined, as it is described in detail in the next chapter.

As a result of recorded FNS and SPS spatiotemporal distributions for given discharges, we analysed the basic phases of each barrier discharge geometry under investigation in more details. For the pre-breakdown Townsend phase the contribution of the α and γ processes, together with the charging of dielectric surfaces lead to distinguishable changes in spatiotemporal discharge development. For example, the charged dielectric cathode in M+D- (metallic anode and dielectric covered cathode) arrangement of asymmetric volume barrier discharge is clearly an additional source of 11 eV electrons in comparison to the M-D+ setup in the next half-period of applied sinusoidal voltage waveform. This leads to far faster accumulation of the necessary charge threshold for streamer (ionising wave) propagation. In general, the observed differences between the SPS intensity profiles along the discharge axis and between the corresponding integral intensity growth rates can be explained by different boundary and initial conditions of the discharge development. In the streamer propagation phase, the velocities of the streamer propagation were compared. The highest positive streamer velocity (determined from the spatiotemporal distributions of the FNS signal) is observed in the case of the M-D+ electrode arrangement. The streamer propagates undisturbed towards the metal cathode in the M-D+ arrangement. In all other cases with dielectric cathodes, the deposited positive ions on the cathode dielectric repulse the positive head of the CDIW during its propagation resulting in lower velocities. We also investigated the phase of the transient glow discharge. For the first time, the long lasting (up to 150 ns) layer of the enhanced electric field at the cathode surface was experimentally observed for the M-D+ in air at atmospheric pressure. The thickness of the cathode layer was found to be about 30 μm with the radius of 120 μm . These values supported the simulations done by Braun et al. in [20]. In the decay phase, the decay of the integral SPS signal was found to be the slowest one for M+D-, while the decay rates for the other three electrode configurations were very close to each other. We concluded that the discharge development during the decay phase is determined by the properties of the anode, i.e. an accumulation of negative charge on the surface of the dielectric anode results in a fast decrease in electric field strength within the discharge channel, and consequently, in a faster decay rate as compared with the M+D- electrode arrangement.

These comparative results were completed by a similar study of the sine driven surface barrier discharge in the second article. As a result of our effort, all four basic barrier

discharges driven by sinusoidal voltage were investigated. The electrical current pulse and TCSPC measurements, as well as the ICCD imaging showed clearly different mechanisms in both polarities. In the positive half-period of the applied voltage on the surface electrode a very similar behaviour of the FNS and SPS emissions was observed in comparison to the previously discussed paper. The Townsend phase, positive streamer propagation along the surface and the filament decay were detected. Nevertheless, the transient glow discharge phase was not present as there is no clearly defined cathode edge. In the negative half-period, the rather low spatial resolution led to the issue in discharge mechanism clarification. Only two years later based on the measurements with an improved resolution, we could clarify this issue applying the unified theory of the streamer breakdown as published in [63] (see the commented article in the next chapter). As a first the microscopic positive streamer is created and impacts the cathode. Only then the discharge channel is created and the cathode layer feeds the negative streamer with sufficient current.

The third article describes the effect of the pulse width on the discharge mechanism in the repetitive pulsed barrier discharges in atmospheric pressure N_2/O_2 (0.1 vol. % oxygen in nitrogen gas) mixture. Barrier discharges were powered by high voltage pulses of widths between 10 μs and 200 ns and with the rising and falling slopes of the positive pulse voltage slopes of approximately 250 V/ns. The development of the micro-discharges on rising and falling slopes was recorded by streak and intensified CCD cameras simultaneously. The discharge appearance was magnified using a far-field microscopy. It was shown that the breakdown on the falling slope strongly depends on the selected pulse width. As a result of pulse width variation the starting point of ignition changes and positive and negative streamers occur simultaneously in the falling slope. We clarified that the observed effect is caused by the electric field rearrangement in the gap due to the different positive ion densities related to their gap crossing times. As the pulse width (i.e. the time between the rising and the falling slope breakdown) decreased, a higher densities of the positive ions were still present in the gap from the previous breakdown on the rising slope. The threshold width interval was 1 μs , where the traditional scheme of the positive streamer creation etc., as described in the introduction, completely failed. The free charge was created not at the anode but in the space, few hundreds of microns close to the cathode. Similarly to the surface barrier discharge in the negative half-period, microscopic positive and subsequent negative streamers were detected in the gap, see the figure 1.4. These results delivered further evidence for the unification theory, as described in the next chapter.

The next high-resolution parametric study we accomplished, was the investigation of the influence of the oxygen admixture (in nitrogen gas) onto the behaviour of the filamentary barrier discharges in pulsed regime. The result was published in the fourth selected article. The setup and techniques of investigation were the same as in previous article on pulsed barrier discharges. We investigated the spatiotemporal development and breakdown statistics of filamentary micro-discharges in 1 mm gap. The influence of the O_2 admixture was studied for the range of 0.1 to 20 vol% of O_2 in N_2 . Electrical measurements were recorded, as were simultaneous streak and iCCD images of studied micro-discharges. Additionally, a newly developed electrical analysis based on the equivalent circuit model of the discharge was applied (see further in the third chapter). We made following conclusions based on the detailed quantitative analysis: The pulse current maxima increase with rising O_2/N_2 ratio. Under our conditions an O_2 concentration above 5 vol% leads to a

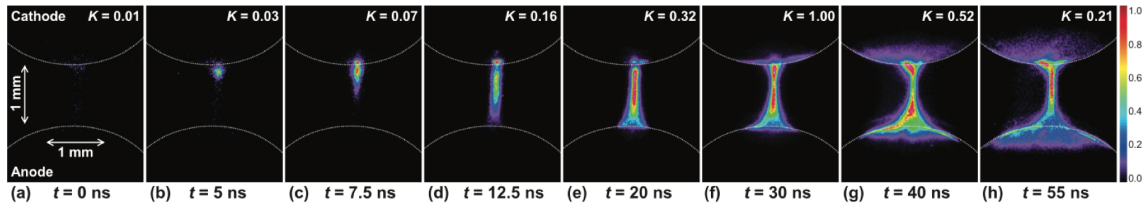


Figure 1.4: ICCD camera record of the micro-discharge emission during the falling slope of the square pulse of duration of $1 \mu\text{s}$. The first luminosity appears $100 \mu\text{m}$ in front of the cathode (part b), it is followed by the creation of the cathode layer due to the impact of the microscopic positive streamer (part c) and the filament is created by the negative streamer (part d). The factor K indicates the intensity scaling with respect to the total maximum in (f). Every picture corresponds to 100 accumulated discharge events. This picture is taken from [60].

breakdown delay which increases the reduced electrical field strength at ignition. The discharge current, the emission durations and the transferred charges all decrease with rising O_2/N_2 ratio. The discharge channel emission diameter increases with the O_2/N_2 ratio, the concentration of 5 vol% is also a threshold value here. The streamer propagation velocities rise with the O_2/N_2 ratio. Because of the steep voltage rise in pulsed operation even a short breakdown delay has a strong influence on the reduced electric field strength in the gap. In other words, an increase in the amount of electronegative O_2 - which delays the breakdown inception - has a significant impact on the discharge physics, apart from the influence of the effective collisional quenching of excited N_2 states by O_2 . These results were explained by the properties of oxygen (e.g. electron trapping and collisional quenching which reduce the background ionisation before breakdown) interplaying with the rapid voltage increase during the pulse slope.

The last, fifth, article in this section focuses on the memory effects in the pulsed barrier discharges. We investigated the influence of the pulse width on the pre-phase and the subsequent breakdown of pulsed barrier discharge in 0.1 vol% O_2 in N_2 at atmospheric pressure with a 10 kV pulse amplitude and a 10 kHz repetition rate. This article further deepened, using the fluid computer modelling (contribution of M. M. Becker and D. Loffhagen), the understanding of the previously published Letter paper [60], the third paper in this commented section. The deviations from the classical chain of the gas breakdown scenario were described and clarified by the gas pre-ionisation. Furthermore, we completed the experimental analysis by the high-resolution TCSPC and, taking the advantage of the Poissonian statistical nature of this technique, a signal recording with uniquely large dynamical range (six orders of magnitude) was constructed. In particular, this approach enabled a detailed detection of the SPS signal which was locally generated by the accelerated residual electrons in the first nanoseconds of the falling slope of the applied voltage for the $10 \mu\text{s}$ pulse widths. Results of the computer modelling were in agreement with this hypothesis.

As a result of the quantitative parametrical analysis, four distinct breakdown regimes were identified, depending on pause times (pulse widths) between the barrier discharges at the rising and falling slopes (specified by t_{pulse}) and ranging from ‘classical’ mechanism

of cathode-directed (positive) streamer propagation, to no streamer propagation at all for sub- μs pause times. All regimes were determined by their different behaviours in their pre-phases. For $99.8 \mu\text{s} \geq t_{\text{pulse}} \geq 20 \mu\text{s}$, no peculiarities in the pre-phase were observed, while the breakdown featured an exponential increase in the SPS (of N_2) emission in front of the anode, followed by a propagation of a fast cathode-directed streamer. For pause times between $20 \mu\text{s}$ and $4 \mu\text{s}$ a temporally limited (isolated) diffuse SPS emission was found, as pointed out above. This was correlated to a considerably high residual electron density in the gap, which led to changes in the spatiotemporal barrier discharge development - i.e. the propagation velocity, the streamer inception point and the applied breakdown voltage - but to no general changes in the breakdown characteristics. The discharge behaviour completely changes for pause times in the range of 2 to $1 \mu\text{s}$ where a simultaneous cathode- and anode-directed streamer propagation was observed, starting directly from the pre-phase near the cathode. When the pause time was below $0.5 \mu\text{s}$, no streamer propagation occurred, but a re-ignition of the afterglow of the previous discharge. The results of the modelling quantified in details and supported the previously stated hypothesis that the effects of the pause time are correlated to a change in the pre-ionisation created by the previous discharge. The pre-ionisation is created especially by the residual electrons, positive nitrogen N_2^+ and oxygen O_2^+ ions.

1.3 Barrier discharge channel stratification in argon

Experiments in the asymmetric volume barrier discharge in atmospheric pressure argon revealed the presence of the discharge channel stratification. The striated column is well known from the glow discharges in lower pressure gas mixtures. Here however, we observed a stratification in micrometrical range of the discharge channel created only for a few units of microseconds [64]. Experimental [64] and theoretical [65] (in cooperation with C. Wilke and the computer modelling group at INP Greifswald, i.e. M.M. Becker and D. Loffhagen) efforts were made to clarify this phenomenon in detail. The example of the visual appearance of the striated discharge with its electrical current development is given in Fig. 1.5. Following articles are commented in the following text:

1. **Hoder T**, Loffhagen D, Wilke C, Grosch H, Schäfer J, Weltmann KD and Brandenburg R 2011 Striated microdischarges in an asymmetric barrier discharge in argon at atmospheric pressure *Physical Review E* **84**(4) 046404 [64]
2. Becker M M, **Hoder T**, Brandenburg R and Loffhagen D 2013 Analysis of microdischarges in asymmetric dielectric barrier discharges in argon *Journal of Physics D: Applied Physics* **46** 355203 [65]

We applied correlated ICCD imaging and current measurements together with modern techniques of computer modelling. From the discharge channel images and current pulse features the characteristic macroscopic parameters were determined. The scaling law theory known from low-pressure glow discharge diagnostics was applied in order to describe and explain this phenomenon. The investigated microdischarge is characterized as a transient atmospheric-pressure glow discharge with a stratified column. It can be

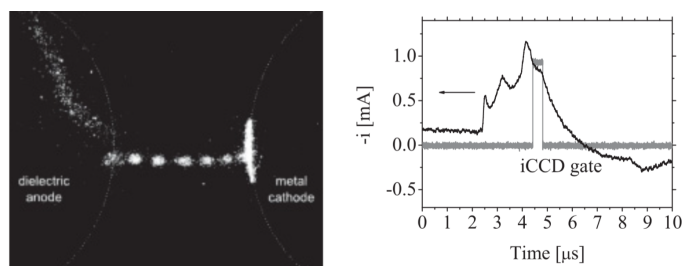


Figure 1.5: Correlated intensified CCD camera and current measurements of the channel stratification in atmospheric pressure argon barrier discharge. The interelectrode gap was 1.5 mm. Argon flow rate is 150 sccm and iCCD gate is 500 ns. This picture is taken from [64].

described by similarity parameters $i/r \approx 0.13$ A/cm, $p \cdot r \approx 5$ Torr·cm and $3 < \lambda/r < 5$ with the current i , pressure p , interval of subsequent striations λ and radius of the plasma channel r . The influence of the small admixture of nitrogen gas was analysed in detail by spectroscopical means and by computing the electron velocity distribution function in multi-term approximation (contribution of D. Loffhagen) for the electric field obtained from the macroscopical parameter λ . An attempt to describe the mechanism of creation of a striated structure is given, based on an established model of the spatial electron relaxation. These computations based on the obtained macroscopic parameters included the electron-electron interaction, which smoothed the electron mean energy profile. Finally based on the previous theoretical efforts, we concluded that a transient Franck-Hertz-like phenomenon takes place [66, 67]. We hypothesised that the source of the non-local electrons is the electron density gradient instability caused by the channel contraction at the metallic cathode, similar to [68]. The occurrence of this instability was connected with the certain over-voltage threshold.

The second article treated the problematic tasks of the channel stratification theoretically (simulations of M.M. Becker), supported by experimental electrical analysis of the discharge. Theoretical and experimental studies of two different discharge modes in asymmetric dielectric barrier discharges in argon at atmospheric pressure have been performed. The first mode appears to be the well-known filamentary micro-discharge with a non-striated positive column whereas the second mode is characterised by discharge instabilities and the appearance of striations. Both experiment and model calculations predict a transition from the first mode to the second mode when the applied voltage amplitude is increased above approximately 2 kV. The reliability of the employed fluid model is confirmed by comparison of the current–voltage characteristics obtained by model calculations and measurements for different applied voltage amplitudes. In general, the results of the model calculations point out that in the second discharge mode the ionisation of excited argon atoms prevents the total recombination of charge carriers between two subsequent discharge events. This leads to the occurrence of the memory from one discharge to the following one, which plays an important role in mode transition.

Furthermore, we were able to exclude a false hypothesis previously considered by us in the first article. The negative differential conductivity action was found by the model

contrary to the previous experimental estimations. The negative differential conductivity is usually a source of the electron ensemble instabilities in gas discharge plasmas [69, 70]. In other words, the theoretical investigations have revealed that the instabilities observed in the experiment at applied voltages, largely exceeding the burning voltage, are potentially caused by the occurrence of negative differential conductivity immediately after the first breakdown in each half-period. It was found that the discharge dynamics at amplitudes in the range from 2 to 2.5 kV is very sensitive with respect to changes in the reaction kinetics of metastable argon atoms Ar[1s5] and Ar[1s3] (Paschen notation). We have also shown that the high rate of chemo-ionisation during the entire temporal evolution prevents the full plasma recombination between subsequent discharge events. Therefore, the characteristics of each breakdown is largely affected by the previous one and re-ignition takes place in a part of the discharge volume only. It has been shown that the role of stepwise ionisation during discharge events increases and the importance of direct ionisation decreases with the transition from the low voltage mode to the high voltage mode. Finally, even though the striations observed in the experiment cannot be reproduced by the fluid model considered, the interplay of direct ionisation and ionisation processes involving excited particles have been found to be a possible reason for the striations observed in the experiment under certain conditions.

Chapter 2

The electric field: a key parameter determination

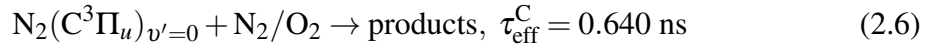
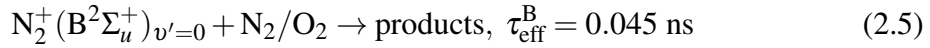
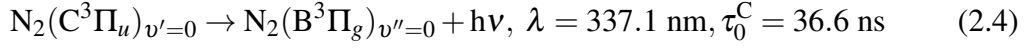
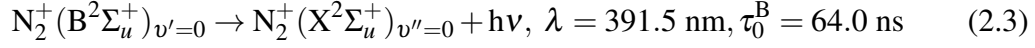
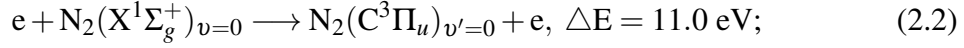
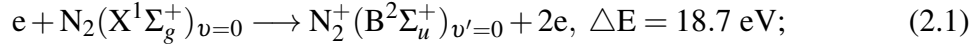
Detailed knowledge of the local and instantaneous electric field strength in gas discharges is crucial for deeper understanding of particular phenomena. The electric field rules the initiated electron-driven chemistry via statistical effects described by the electron energy distribution function. This is important for understanding of the plasma-chemical effects of the particular discharge on its environment. Knowledge of the electric field strength is therefore important for many applications (air-fed ozonizers, air-pollution treatment, plasma-medicine etc.) but also for understanding the atmospheric electricity. In the following sections, the used enhanced method for E/N (gas density reduced electric field strength) determination will be presented together with several case studies of its implementation. The presented and commented work was accomplished by the author during his activities at the INP Greifswald in Germany, Academy of Sciences of the Czech Republic in Prague, Instituto de Astrofísica de Andalucía Granada in Spain, as well as at the Department of physical electronics of the Masaryk University in Brno, Czech Republic. This work was done also in cooperation with Ecole Polytechnique Paris and Pau University in France, as well as Comenius University in Slovakia.

2.1 The method

Researchers have been trying to estimate the mean electron energy or the electric field strength in air-like plasmas already for decades. Typically, the estimation of basic parameters of practically all nitrogen-containing plasmas at different pressures was widely based on the emission of the two above mentioned nitrogen spectral systems, FNS and SPS - dominantly due to the large difference in their excitation potentials which determine their excitation rate coefficients. Thus, also for discharge in atmospheric pressure air, these emissions have been in the focus for a long time as well, especially for streamer discharges [71]. The kinetic scheme enabling the determination of the electric field strength in the discharge using the ratio of FNS and SPS intensities has already been applied by Gallimberti et al. [71] and was further used by others (see [72] and references therein).

The radiation kinetics of these spectral indicators (FNS and SPS) in air at atmospheric pressure is determined dominantly by the following elementary processes: direct elec-

tron impact excitation/ionisation (equations 2.1,2.2), spontaneous radiation (2.3,2.4) and collisional quenching (2.5,2.6) [55, 56]:



In these equations, τ_{eff} stands for the effective lifetime of a given radiative state. It is given by the reduction of the original radiative lifetime τ_0 by collisional quenching [73, 74, 75]. Under the assumption that the direct electron impact excitation process is dominant for the $N_2^+(B^2\Sigma_u^+)_{v'=0}$ and the $N_2(C^3\Pi_u)_{v'=0}$ state, simple balance equations for the densities of the radiative states n_B and n_C can be written. After division and substitution of the densities for measured intensities I_{FNS} and I_{SPS} , one obtains

$$\frac{\frac{dI_B(r,t)}{dt} + \frac{I_B(r,t)}{\tau_{\text{eff}}^B}}{\frac{dI_C(r,t)}{dt} + \frac{I_C(r,t)}{\tau_{\text{eff}}^C}} = R_{FNS/SPS}(E/N). \quad (2.7)$$

Here, $R_{FNS/SPS}(E/N)$ is the ratio, which is an unambiguous rising function of E/N . This calibration curve, connecting the measured intensities and the electric field, can be determined theoretically or experimentally [76, 77].

The problem is that for precise determination of the electric field strength in a streamer discharge a sub-nanosecond-resolved recording of the FNS and SPS emissions is necessary [78, 79, 80, 72, 81]. These emissions have an ultra-short shift between their maxima, given by the electric field waveform and, of course, the different excitation potentials of the radiative states. This has to be taken into account when applying this method for the electric field determination in fast discharges (coronas, barrier discharges or Sprite streamers in air). We clarified this issue in detail in the following commented article:

- **Hoder T**, Bonaventura Z, Bourdon A and Šimek M 2015 Sub-nanosecond delays of light emitted by streamer in atmospheric pressure air: Analysis of $N_2^+(C^3\Pi_u)_{v'=0}$ and $N_2(C^3\Pi_u)_{v'=0}$ emissions and fundamental streamer structure *Journal of Applied Physics* **117** 073302 [72]

In this article, theoretical analysis of ultra-short phenomena occurring during the positive streamer propagation in atmospheric pressure air is presented. Motivated by our experimental results obtained using TCSPC with a precision of tens-of-picoseconds and tens-of-microns, it is shown that, when the streamer head passes a spatial coordinate, emission maxima from $N_2^+(C^3\Pi_u)_{v'=0}$ and $N_2(C^3\Pi_u)_{v'=0}$ radiative states follow with different delays. We reported that these different delays are caused by differences in the

dynamics of populating the radiative states, due to different excitation and quenching rates. Associating the position of the streamer head with the maximum value of the self-enhanced electric field, a delay of 160 ps was experimentally found for the peak emission of the first negative system of N_2^+ ion. In surprising contrast to the highly nonlinear behaviour of streamer events, a linear dependence was found using 2D axi-symmetric simulations as well as 1D analytic models (contributions of Z. Bonaventura and A. Bourdon) for the emission maxima delays as a function of the streamer radius to velocity ratio r/v . We concluded that the coupling of the delay and the r/v parameter represents an intrinsic characteristic of the streamer head and we proposed an analytical model for this coupling. A delay dilatation of few tens of picoseconds was observed experimentally on early-stage streamers and the general mechanism of this phenomenon is clarified theoretically. The dilatation of these delays of few tens-of-picoseconds during the early-stage streamer evolution was obtained using the proposed model in good agreement with experimental findings. We have shown that the SPS delay can reach the value of up to 400 ps at given conditions, which can cause an error in the discharge analysis by correlating electrical measurements (current and voltage waveforms for instantaneous power and energy estimation) to the early-stage streamer emission development only. As we have shown in this article, the detected emission only represents populations of excited states formed behind the running streamer head, giving only delayed information about the streamer head position. We concluded that it is reasonable to expect that similar phenomena occur in other streamer-mechanism driven discharges, too (e.g. plasma jets or transient sparks in helium or argon mixtures with air).

Furthermore, for the first time, based on the results of a 2D axi-symmetric model, a spectrometric representation of the whole streamer head area was visualised for subsequent picosecond moments (contribution of M. Šimek). It is shown that for short delays, the FNS emission peaks at the axis of the streamer, while several tens of picoseconds later more complex FNS intensity distributions appear. Also, by understanding the structure of emission spectra in the streamer head, one can assess that the radial averaging of the streamer emission will cause smaller distortion of the further processed signal in comparison with the axial signal integration. This last finding is important for further data processing of spectroscopic data for E/N determination through the ratio method.

2.2 Trichel pulses in negative corona in air: a unification theory of the gas discharge mechanism

In this section, the issue of the discharge mechanism of negative corona Trichel pulses is addressed [25, 82]. The mechanism of Trichel pulses in negative corona discharge in atmospheric pressure air has been a controversial topic already for decades. It was also one of the last critical issues to be understood for the completion of the unification model of high-pressure gas breakdown. At gas pressures above roughly 10 kPa, the sequence of events leading to an arc formation consists of the bridging of the gap by primary streamers, and the subsequent heating of the initial channel created by the streamers [1, 82]. The transition between these two stages is determined by the formation of an active cathode spot capable of feeding an increasing current of electrons into the discharge channel.

The mechanism for cathode spot formation still remains somewhat obscure, and it is the important and still missing segment in a unified theory consistently integrating the extensive results pertaining to the streamer-initiated breakdown phenomena: Except for the pre-breakdown phenomena in negative corona gaps and for cathode spot formation by a breakdown of cathode sheaths of pulsed high-pressure discharges [83], the primary-streamer arrival to the cathode is accepted to be a turning point in the streamer-initiated-breakdown development leading to the final arc formation. In the exceptional cases mentioned, cathode spot formation is related to fast phenomena ($\sim 0.1\text{--}1$ ns) inside of a narrow (~ 0.1 mm) high-field region in the cathode vicinity. Because of an apparent technical difficulties of viewing such a microscopic area with a sub-nanosecond time resolution, the formation of cathode-directed streamers in such very narrow cathode regions is obviously not considered. This causes the mentioned inconsistency in theory concerning cathode spot formation in high pressure discharges. We approached this topic in the following two papers:

1. **Hoder T**, Černák M, Paillol J, Loffhagen D and Brandenburg R 2012 High-resolution measurements of the electric field at the streamer arrival to the cathode: A unification of the streamer-initiated gas-breakdown mechanism *Physical Review E* **86**(5) 055401 [63]
2. **Hoder T**, Loffhagen D, Voráč J, Becker M M and Brandenburg R 2016 Analysis of the electric field development and the relaxation of electron velocity distribution function for nanosecond breakdown in air *Plasma Sources Science and Technology* **25** 025017 [84]

In the first article, from the measured FNS and SPS recordings with spatiotemporal distribution of 10 ps and 10 μm , we revealed a fast microscopical streamer process including both positive and negative streamer occurrence. We estimated the velocity of the positive and negative streamers to be 6×10^4 and 7×10^5 m/s, respectively. The positive streamer electric field was determined to be 8×10^6 V/m and even a higher field at the created cathode layer, both in agreement with results of numerical modelling [19, 20]. The characteristics of the cathode-directed streamer as well as the measured spatiotemporal development of its electric field, indicated that the ionisation processes leading to the fast current rise to the Trichel pulse maximum are associated with the formation of a microscopic positive streamer in the immediate vicinity of the cathode. It is important to mention that this fact was not considered in a great majority of recent computer simulations. We have supposed that such phenomena occur in many practical situations and their consideration offers the attractive feature of the theoretical unification of all streamer-initiated breakdown processes. As a first step to such unification we claimed that the results presented here indicate that any streamer-initiated breakdown phenomenon in a discharge gap with a highly stressed cathode (e.g. negative corona gap) is always associated with the positive-streamer formation in the vicinity of the cathode surface. This was confirmed by the author for barrier discharges with different pulse width in [60] and sinusoidal driven surface barrier discharges [59].

In the second article (invited contribution), we improved the above mentioned approach, confirmed the previously obtained findings and clarified the effect of the gas heating using

SPS spectra thermometry (spectroscopic simulation contributed by J. Voráč). Also the charge transfer in the gap and in the direct microscopic vicinity of the negative electrode was clarified using analytical models and also using computer simulations (contribution of M.M. Becker). Finally, the spatiotemporal relaxation of the electron velocity distribution function for electric fields obtained in the experiment was computed (contribution of D. Loffhagen) using unique multi-term solving of the Boltzmann equation. These simulations confirmed the local field approximation for the electron ensemble which is crucial for the application of the ratio method for E/N determination in highly transient plasmas with strong electric field gradients.

2.3 Barrier discharge on the dielectric surface

Coplanar barrier discharge is widely used for surface treatment of various materials. It is a discharge generated on the surface of dielectrics in which both electrodes are embedded. The so called Diffuse Coplanar Surface Barrier Discharge developed at the Department of Physical Electronics in the team of prof. M. Černák is applied in several plasma related research and development areas. As the coplanar discharge propagates dominantly on the surface, the created residual surface charge has a strong influence on the subsequent discharge propagation [23, 85, 86, 87]. We approached this topic using discharge arrangement which modelled such situation. There, two surface streamers of the same polarity propagated on the dielectric surface close to each other. The following invited article described our results:

- **Hoder T**, Synek P, Chorvát D, Ráhel J, Brandenburg R and Černák M 2017 Complex interaction of subsequent surface streamers via deposited charge: a high-resolution experimental study *Plasma Physics and Controlled Fusion* **59** 074001 [88]

We have recorded the development of two subsequent surface microdischarges in air by TCSPC and intensified CCD camera technique with high spatiotemporal resolution. We performed also a precise electrical measurements. Using special current probe inspired by setup from [89] and implementing the method of Pipa et al. [90, 91] (see also the last chapter) we quantified the transferred charge to the dielectric surface. The deposited surface charge from the first microdischarge significantly affects the pattern of the second event. Subsequently, the residual charge remaining behind the massive second microdischarge significantly biases the effective electric field in the gap as it was obtained from the precise electric measurements. We have observed multiple phenomena of surface streamer branching, reconnection and deceleration of streamer propagation on surfaces charged with the same polarity. A unique spatiotemporal distribution of the reduced electric field strength was obtained using the FNS/SPS ratio method which can be further used for the determination of the streamer-initiated surface plasma-chemistry similarly as we have done for volume streamers in [92]. The peak values of the positive streamers were 1200 Td for the presumably uncharged dielectric surface and even higher for the charged one. These high values were recently obtained also using hybrid and fluid modelling [93]. We hope that the understanding of such discharge behaviour and of the generated close-surface plasma-chemistry may lead to better design of surface barrier discharges used for industrial plasma treatment in air.

2.4 Barrier discharge streamer as an atmospheric lightning analog

In our further application of the electric field determination method from the spectroscopic signatures of FNS and SPS, we approached the topic of streamer dynamics at lower pressures - similar to the lower stratosphere where the ozone layer is placed. Such early stage streamers are the first stages of the larger discharges, they are preceding the creation of the leader discharge which creates the lightning phenomena [6, 7]. We experimentally determined the electric field radially and temporally resolved and computed the generated plasma-chemistry using plasma-chemical kinetic model (contribution of F.J. Gordillo-Vázquez). Our results are described in detail in the following article:

- **Hoder T, Šimek M, Bonaventura Z, Prukner V and Gordillo-Vázquez F J** 2016 Radially and temporally resolved electric field of positive streamers in air and modelling of the induced plasma chemistry *Plasma Sources Science and Technology* **25** 045021 [92]

The reduced electric field strength distribution peaked at 500 Td, with a temporal profile corresponding to the classical theoretical results on streamer structure by Kulikovskiy et al. [94], which is also used as a tool for extrapolation to low field values, see Fig. 2.1. Kulikovskiy's analytical model was confirmed both numerically [79, 72, 94] and experimentally [95]. The influence of the different sets of quenching constant on the resulting electric field strength is presented on sub-nanosecond resolved data for the first time, further improving the art of implementation of the ratio method.

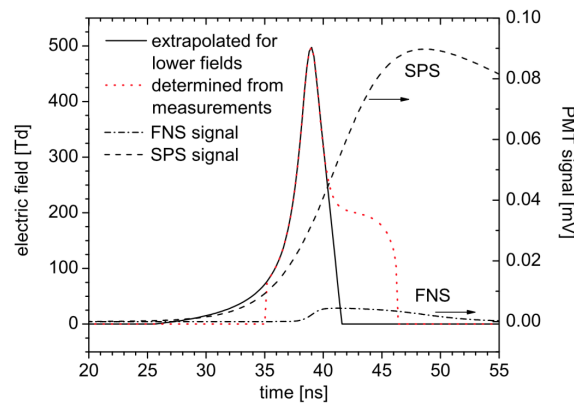


Figure 2.1: Recorded FNS and SPS sub-nanosecond signals for the 4 torr streamer in air, reconstructed E/N waveform and the extrapolation according to the Kulikovskiy analytical model [94]. This picture is taken from [92].

Analysing the results of kinetic modelling we found that the production of ozone is negligible, while that of nitride oxide was considerably enhanced with respect to its ambient value. We found that streamers produced under given conditions (4 torr or 37 km altitude) are able to seed the air ahead of Blue Jets (a type of stratospheric transient luminous event)

with significant transient concentrations of chemical species such as $O(^1D)$ and $N(^2D)$, which contribute to fast heating and, ultimately, to the streamer to leader transition.

2.5 The spark discharge mechanism in air

Another discharge mechanism we addressed in our experiments was the spark discharge, as it is the direct transition between the non-thermal streamer-ruled and thermalised arc-like discharge mechanisms. In our investigations, apart from the SPS and FNS signals, the emission of the atomic lines of oxygen and nitrogen were recorded by the TCSPC, too. We published our findings in [96].

We obtained the spatiotemporal distribution of the reduced electric field strength during the primary streamer phase of the transient spark peaking at approx. 300 Td. This value is considerably lower than that in the previous case. We concluded that this is due to the higher residual ionisation of the gas after it has been exposed to the thermalised plasma at high repetition frequency. Typically, in pre-ionised gas sufficient amount of electrons is for disposal and so a high electric field gradient does not develop. The transition from streamer to spark proceeds very fast within about 10 ns for the case with a current pulse repetition rate in the range 8-10 kHz. This is attributed to memory effects, leading to a low net electron attachment rate and faster propagation of the secondary streamer. We concluded that gas heating, accumulation of species such as oxygen atoms from the previous spark pulses, as well as the generation of charged particles by stepwise ionisation can play an important role contributing to this fast streamer-to-spark transition. The emission of the atomic spectral lines of nitrogen and oxygen was detected dominantly during the phase of discharge channel thermalisation indicating an increasing dissociation level of originally molecular gas.

Moreover, we addressed the issue of the secondary streamer and tried to determine also the electric field in it. The conditions created by the primary streamer however, prevented our method to work with sufficient precision, so we could only comment on the maximum threshold which was not exceeded.

Chapter 3

Electrical diagnostics: an important supportive method

Electrical measurement of discharge current and voltage waveforms is a classical and sometimes the easiest way to access the dissipated energy or estimate the electron density in the generated plasma [48]. In the case of streamer-initiated discharges however, the temporal timescales go to the sub-nanosecond level and the current amplitude in some pre-breakdown phenomena is in the order of few units of micro-amperes. In the following sections, we briefly describe some enhanced methodology and techniques we applied as supportive means which can confirm spectroscopically obtained results.

3.1 Electrical current probes and their performance

The first problem, as noted above, is the design of the proper setup which is able to detect low and fast changing signals. We adopted the methodology proposed in [89, 97] where a so called coaxial design of the current probe was used. Similar experiments were done also in [98] or [99] where it was further improved with the statistical analysis. Coaxial setup minimises the noise and oscillations in the signal due to the external influences. Only such an enhanced setup combined with high-tech oscilloscopes with sufficient bandwidth can lead to results capturing the fine features of the current signal under investigation. Such a setup was applied in our experiments also, during the investigation of both coronas [63], and barrier discharges [88, 92]. The step at the leading edge of the current pulse of negative corona Trichel discharges in atmospheric pressure air can be resolved, which is a sign of well adjusted electrical measurements [63, 72]. Study of this extremely fast feature of the current pulse enabled a deeper analysis of the fundamental mechanism of the Trichel pulse [82]. We correlated the current measurements with optical recordings and electric field development for the first time in [63] and contributed to the experimental understanding of the Trichel pulse corona discharge.

3.2 An equivalent circuit approach

In the case of electrical characterisation of barrier discharges, one has to deal with the capacitive nature of the system. The current and voltage measured in the external circuit are not the real values physically present in the gas gap as a plasma parameters [50, 100]. This makes the analysis more complex in comparison to the corona or spark discharges where the electrodes are in direct electrical contact with the plasma. Typically, an equivalent circuit has to be applied using the Kirchhoff equations to decouple the net discharge characteristics from the recorded signals [100, 101]. The net discharge current, gas gap voltage, net transferred charge and instantaneous power can be obtained. The gas gap voltage is of special importance, as it gives the temporal development of the value of the average electric field in the gas gap, if divided by the gap size. This fact can be used to calibrate the electric field determined spectroscopically using FNS/SPS ratio method as described earlier in this text. The spectroscopically obtained spatiotemporal distribution of the electric field strength can be integrated over the space for each time giving temporal development to the field comparable to electrical measurements. This was successfully applied by the author and his colleagues in [88, 92]. For the above described approach however, one has to know all the parameters of the analysed equivalent circuit. The effective capacitances of the discharge system are of the main importance.

With A. V. Pipa, we presented such an approach for pulsed barrier discharges and improved the methodology for the necessary parameter determination - the effective discharge capacitances. It was published in the following articles:

1. Pipa A V, **Hoder T**, Koskulics J, Schmidt M and Brandenburg R 2012 Experimental determination of dielectric barrier discharge capacitance *Review of Scientific Instruments* **83** 075111 [90]
2. Pipa A V, Koskulics J, Brandenburg R and **Hoder T** 2012 The simplest equivalent circuit of a pulsed dielectric barrier discharge and the determination of the gas gap charge transfer *Review of Scientific Instruments* **83** 115112 [91]

The determination of electrical parameters (such as instantaneous power, transferred charge, and gas gap voltage) in barrier discharge reactors relies on estimates of key capacitance values (and their accuracy, see Fig. 3.1 [102], contribution of the author). We addressed this topic in the first article.

In the classic large-scale sinusoidal-voltage driven discharges, also known as silent or ozonizer discharge, capacitance values can be determined from a charge-voltage (Q-V) plot, also called Lissajous figure. For miniature laboratory reactors driven by fast pulsed voltage waveforms with sub-microsecond rise time, the capacitance of the dielectric barriers cannot be evaluated from a single Q-V plot because of the limited applicability of the classical theory. Theoretical determination can be problematic due to electrode edge effects, especially in the case of asymmetrical electrodes. We stress the fact that the lack of reliable capacitance estimates leads to a “capacitance bottleneck” that obstructs the determination of other discharge electrical parameters in fast-pulsed reactors. We suggest to obtain the capacitance of dielectric barriers from a plot of the maximal charge versus maximal voltage amplitude (Q_{\max} - V_{\max} plot) in a manner analogous to the classical

approach. We examined this method using measurements of current and voltage waveforms of a coaxial discharge reactor in argon at 100 mbar driven by square voltage pulses with a rise time of 20 ns and with different voltage amplitudes up to 10 kV. Additionally, we confirmed the applicability of the method also for the data reported in literature measured at 1 bar of nitrogen-oxygen gas mixtures and xenon.

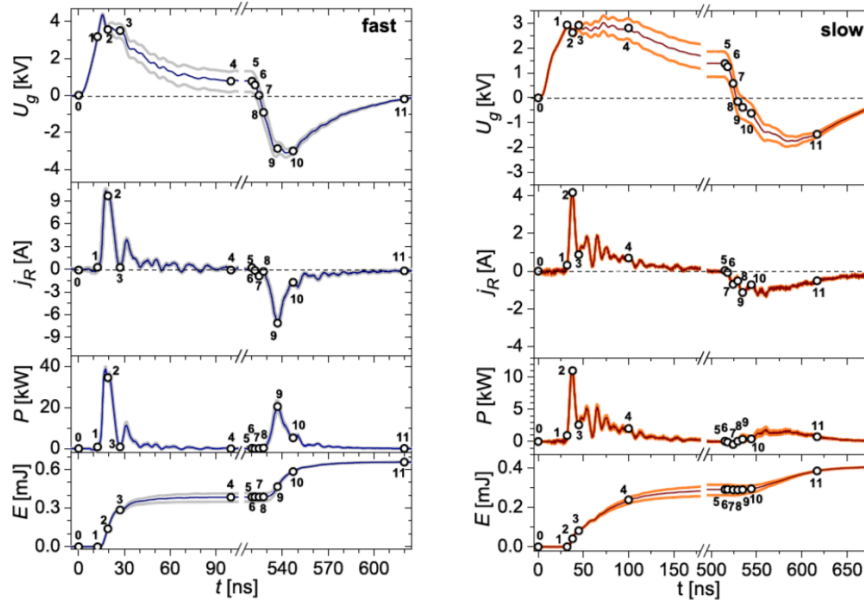


Figure 3.1: The influence of the effective capacitance values onto the further discharge parameters using the simplest equivalent circuit. Gas gap voltage $U_g(t)$, discharge current $j_R(t)$, instantaneous electrical power $P(t)$ and energy $E(t)$ coupled into discharge for fast and slow nanosecond applied voltage switches. See [102] for more details. This picture is taken from [102], contribution of the author.

In the second article, we have reviewed the concept of the simplest equivalent circuit for barrier discharges in general. We show that the approach is consistent with experimental data measured either in large-scale sinusoidal-voltage driven or miniature pulse-voltage driven discharges. An expression for the charge transferred through the gas gap $q(t)$ is obtained with an accurate account for the displacement current and the values of discharge reactor capacitance. This enabled (1) a significant reduction of experimental error in the determination of $q(t)$ in pulsed barrier discharges, (2) the verification of the classical electrical theory of ozonizers about maximal transferred charge q_{\max} , and (3) the development of a graphical method for the determination of q_{\max} from charge-voltage characteristics measured under pulsed excitation.

References

- [1] Meek J and Craggs J 1978 *Electrical Breakdown of Gases* (John Wiley and Sons Ltd.) ISBN 0471995533
- [2] Becker K, Kogelschatz U, Schoenbach K and Barker R 2004 *Non-Equilibrium Air Plasmas at Atmospheric Pressure* (CRC Press, IoP) ISBN 0750309628
- [3] Kogelschatz U 2004 *Plasma Physics and Controlled Fusion* **46** B63 URL <http://stacks.iop.org/0741-3335/46/i=12B/a=006>
- [4] Raizer Y P 2001 *Gas Discharge Physics* (Springer-Verlag) ISBN 978-3540194620
- [5] Bazelyan E M and Raizer Y P 2000 *Lightning Physics and Lightning Protection* (CRC Press, IoP) ISBN 0750304774
- [6] Pasko V P 2007 *Plasma Sources Science and Technology* **16** S13 URL <http://stacks.iop.org/0963-0252/16/i=1/a=S02>
- [7] Pasko V P 2008 *Plasma Physics and Controlled Fusion* **50** 124050 URL <http://stacks.iop.org/0741-3335/50/i=12/a=124050>
- [8] Wijsman R A 1949 *Phys. Rev.* **75**(5) 833–838 URL <https://link.aps.org/doi/10.1103/PhysRev.75.833>
- [9] Hodges R V, Varney R N and Riley J F 1985 *Phys. Rev. A* **31**(4) 2610–2620 URL <https://link.aps.org/doi/10.1103/PhysRevA.31.2610>
- [10] Phelps A V and Petrovic Z L 1999 *Plasma Sources Science and Technology* **8** R21 URL <http://stacks.iop.org/0963-0252/8/i=3/a=201>
- [11] Townsend J S 1915 *Electricity in Gases* (Oxford University Press) ISBN 9785878309981
- [12] Rogowski W 1928 *Archiv für Elektrotechnik* **20** 99–106 ISSN 1432-0487 URL <https://doi.org/10.1007/BF01659954>
- [13] Raether H 1939 *Zeitschrift für Physik* **112** 464–489 ISSN 0044-3328 URL <https://doi.org/10.1007/BF01340229>
- [14] Kip A F 1938 *Phys. Rev.* **54**(2) 139–146 URL <https://link.aps.org/doi/10.1103/PhysRev.54.139>

- [15] Loeb L B and Kip A F 1939 *Journal of Applied Physics* **10** 142–160 URL <http://dx.doi.org/10.1063/1.1707290>
- [16] Loeb L B 1936 *Rev. Mod. Phys.* **8**(3) 267–293 URL <https://link.aps.org/doi/10.1103/RevModPhys.8.267>
- [17] Marode E, Djermoune D, Dessante P, Deniset C, Ségur P, Bastien F, Bourdon A and Laux C 2009 *Plasma Physics and Controlled Fusion* **51** 124002 URL <http://stacks.iop.org/0741-3335/51/i=12/a=124002>
- [18] Ebert U, Montijn C, Briels T M P, Hundsdorfer W, Meulenbroek B, Rocco A and van Veldhuizen E M 2006 *Plasma Sources Science and Technology* **15** S118 URL <http://stacks.iop.org/0963-0252/15/i=2/a=S14>
- [19] Odrobina I and Černák M 1995 *Journal of Applied Physics* **78** 3635–3642 URL <http://dx.doi.org/10.1063/1.359940>
- [20] Braun D, Gibalov V and Pietsch G 1992 *Plasma Sources Science and Technology* **1** 166 URL <http://stacks.iop.org/0963-0252/1/i=3/a=004>
- [21] Levko D and Raja L L 2016 *Journal of Applied Physics* **119** 153301 URL <http://dx.doi.org/10.1063/1.4947055>
- [22] Kogelschatz U 2003 *Plasma Chemistry and Plasma Processing* **23** 1–46 ISSN 1572-8986 URL <https://doi.org/10.1023/A:1022470901385>
- [23] Guikema J, Miller N, Niehof J, Klein M and Walhout M 2000 *Phys. Rev. Lett.* **85**(18) 3817–3820 URL <https://link.aps.org/doi/10.1103/PhysRevLett.85.3817>
- [24] Janda M, Machala Z, Niklová A and Martišovits V 2012 *Plasma Sources Science and Technology* **21** 045006 URL <http://stacks.iop.org/0963-0252/21/i=4/a=045006>
- [25] Trichel G W 1938 *Phys. Rev.* **54**(12) 1078–1084 URL <https://link.aps.org/doi/10.1103/PhysRev.54.1078>
- [26] Hagelaar G J M and Pitchford L C 2005 *Plasma Sources Science and Technology* **14** 722 URL <http://stacks.iop.org/0963-0252/14/i=4/a=011>
- [27] Pancheshnyi S, Bordage M C, Chaudhury B, Chowdhury S, Hagelaar G J M, Pitchford L C, Puech V, Bartschat K, Morgan W L, Viehland L, Zatsarinny O, d’Urquijo J, Castrejon-Pita A A, Hernandez-Avila J L, Basurto E, Bray I, Fursa D V, Biagi S F, Quantemol, Alves L L, Ferreira C M, Kochetov I, Napartovich A, Itikawa Y, Stauffer A, Brion C and van Dijk J 2009 Plasma data exchange project <https://fr.lxcat.net> accessed: 2017-09-12
- [28] Pitchford L C, Alves L L, Bartschat K, Biagi S F, Bordage M C, Bray I, Brion C E, Brunger M J, Campbell L, Chachereau A, Chaudhury B, Christophorou L G, Carbone E, Dyatko N A, Franck C M, Fursa D V, Gangwar R K, Guerra V, Haefliger

- P, Hagelaar G J M, Hoesl A, Itikawa Y, Kochetov I V, McEachran R P, Morgan W L, Napartovich A P, Puech V, Rabie M, Sharma L, Srivastava R, Stauffer A D, Tennyson J, de Urquijo J, van Dijk J, Viehland L A, Zammit M C, Zatsarinny O and Pancheshnyi S 2017 *Plasma Processes and Polymers* **14** 1600098–n/a ISSN 1612-8869 1600098 URL <http://dx.doi.org/10.1002/ppap.201600098>
- [29] Pancheshnyi S, Eismann B, Hagelaar G J M and Pitchford L C 2008 Computer code *zdplaskin* <http://www.zdplaskin.laplace.univ-tlse.fr> University of Toulouse, LAPLACE, CNRS-UPS-INP, Toulouse, France, accessed: 2017-09-12
- [30] Eliasson B, Hirth M and Kogelschatz U 1987 *Journal of Physics D: Applied Physics* **20** 1421 URL <http://stacks.iop.org/0022-3727/20/i=11/a=010>
- [31] Šimek M and Člupek M 2002 *Journal of Physics D: Applied Physics* **35** 1171 URL <http://stacks.iop.org/0022-3727/35/i=11/a=311>
- [32] Pekárek S 2015 *Plasma Chemistry and Plasma Processing* **35** 705–719 ISSN 1572-8986 URL <https://doi.org/10.1007/s11090-015-9628-7>
- [33] Šimor M, Ráhel J, Vojtek P, Černák M and Brablec A 2002 *Applied Physics Letters* **81** 2716–2718 URL <http://dx.doi.org/10.1063/1.1513185>
- [34] Wagner H E, Brandenburg R, Kozlov K, Sonnenfeld A, Michel P and Behnke J 2003 *Vacuum* **71** 417 – 436 ISSN 0042-207X , Symposium on Plasma Surface Engineering at the Spring Meeting of the German Physical Society, Regensburg, Germany, March 11-15 2002 URL <http://www.sciencedirect.com/science/article/pii/S0042207X02007650>
- [35] Morent R, Geyter N D, Verschuren J, Clerck K D, Kiekens P and Leys C 2008 *Surface and Coatings Technology* **202** 3427 – 3449 ISSN 0257-8972 URL <http://www.sciencedirect.com/science/article/pii/S0257897207012704>
- [36] Kim H H 2004 *Plasma Processes and Polymers* **1** 91–110 ISSN 1612-8869 URL <http://dx.doi.org/10.1002/ppap.200400028>
- [37] Jōgi I, Stamate E, Irimiea C, Schmidt M, Brandenburg R, Holub M, Bonislawski M, Jakubowski T, Kääriäinen M L and Cameron D C 2015 *Fuel* **144** 137 – 144 ISSN 0016-2361 URL <http://www.sciencedirect.com/science/article/pii/S0016236114012344>
- [38] Starikovskiy A and Aleksandrov N 2013 *Progress in Energy and Combustion Science* **39** 61 – 110 ISSN 0360-1285 URL <http://www.sciencedirect.com/science/article/pii/S0360128512000354>
- [39] Moreau E 2007 *Journal of Physics D: Applied Physics* **40** 605 URL <http://stacks.iop.org/0022-3727/40/i=3/a=S01>
- [40] Corke T C, Enloe C L and Wilkinson S P 2010 *Annual Review of Fluid Mechanics* **42** 505–529 URL <https://doi.org/10.1146/annurev-fluid-121108-145550>

- [41] von Woedtke T, Reuter S, Masur K and Weltmann K D 2013 *Physics Reports* **530** 291 – 320 ISSN 0370-1573 plasmas for Medicine URL [//www.sciencedirect.com/science/article/pii/S0370157313001634](http://www.sciencedirect.com/science/article/pii/S0370157313001634)
- [42] Williams E R 2009 *Atmospheric Research* **91** 140 – 152 ISSN 0169-8095 13th International Conference on Atmospheric Electricity URL <http://www.sciencedirect.com/science/article/pii/S0169809508001804>
- [43] Winkler H and Notholt J 2015 *Journal of Atmospheric and Solar-Terrestrial Physics* **122** 75 – 85 ISSN 1364-6826 URL <http://www.sciencedirect.com/science/article/pii/S1364682614002430>
- [44] Gordillo-Vázquez F J 2008 *Journal of Physics D: Applied Physics* **41** 234016 URL <http://stacks.iop.org/0022-3727/41/i=23/a=234016>
- [45] Gordillo-Vázquez F J 2010 *Journal of Geophysical Research: Space Physics* **115** n/a–n/a ISSN 2156-2202 a00E25 URL <http://dx.doi.org/10.1029/2009JA014688>
- [46] Hippler R, Kersten H, Schmidt M and Schoenbach K H (eds) 2008 *Low Temperature Plasmas: Fundamentals, Technologies and Techniques* (Wiley-VCH) ISBN 978-3-527-40673-9
- [47] Eliasson B and Kogelschatz U 1991 *IEEE Transactions on Plasma Science* **19** 309–323 ISSN 0093-3813
- [48] Buss K 1932 *Archiv für Elektrotechnik* **26** 261–265 ISSN 1432-0487 URL <https://doi.org/10.1007/BF01657192>
- [49] Siemens W 1857 *Poggendorff's Ann. Phys. Chem.* **102** 66
- [50] Manley T C 1943 *Trans. Electrochem. Soc.* **84** 83
- [51] Samoilovich V G, Gibalov V and Kozlov K V 1997 *Physical Chemistry of the Barrier Discharge* (DVS-Verlag, Duesseldorf) ISBN 3871557447
- [52] Heuser C 1985 *Zur Ozonerzeugung in Elektrischen Gasentladungen* Ph.D. thesis RWTH Aachen, Germany
- [53] Kozlov K, Shepeliuk O and Samoilovich V 1995 Spatio-temporal evolution of the dielectric barrier discharge channels in air at atmospheric pressure *11th Int. Conf. on Gas Discharges and their Applications* vol 2 (Tokyo, Japan) p 142
- [54] Braun D, Kuechler U and Pietsch G 1991 *Journal of Physics D: Applied Physics* **24** 564 URL <http://stacks.iop.org/0022-3727/24/i=4/a=007>
- [55] Kozlov K V, Wagner H E, Brandenburg R and Michel P 2001 *Journal of Physics D: Applied Physics* **34** 3164 URL <http://stacks.iop.org/0022-3727/34/i=21/a=309>

- [56] Kozlov K V and Wagner H E 2007 *Contributions to Plasma Physics* **47** 26–33 ISSN 1521-3986 URL <http://dx.doi.org/10.1002/ctpp.200710005>
- [57] Hoder T, Brandenburg R, Basner R, Weltmann K D, Kozlov K V and Wagner H E 2010 *Journal of Physics D: Applied Physics* **43** 124009 URL <http://stacks.iop.org/0022-3727/43/i=12/a=124009>
- [58] Hoder T, Šíra M, Kozlov K V and Wagner H E 2008 *Journal of Physics D: Applied Physics* **41** 035212 URL <http://stacks.iop.org/0022-3727/41/i=3/a=035212>
- [59] Grosch H, Hoder T, Weltmann K D and Brandenburg R 2010 *The European Physical Journal D* **60** 547–553 ISSN 1434-6079 URL <https://doi.org/10.1140/epjd/e2010-00239-8>
- [60] Hoder T, Höft H, Kettlitz M, Weltmann K D and Brandenburg R 2012 *Physics of Plasmas* **19** 070701 URL <http://dx.doi.org/10.1063/1.4736716>
- [61] Höft H, Kettlitz M, Hoder T, Weltmann K D and Brandenburg R 2013 *Journal of Physics D: Applied Physics* **46** 095202 URL <http://stacks.iop.org/0022-3727/46/i=9/a=095202>
- [62] Höft H, Kettlitz M, Becker M M, Hoder T, Loffhagen D, Brandenburg R and Weltmann K D 2014 *Journal of Physics D: Applied Physics* **47** 465206 URL <http://stacks.iop.org/0022-3727/47/i=46/a=465206>
- [63] Hoder T, Černák M, Paillol J, Loffhagen D and Brandenburg R 2012 *Phys. Rev. E* **86**(5) 055401 URL <https://link.aps.org/doi/10.1103/PhysRevE.86.055401>
- [64] Hoder T, Loffhagen D, Wilke C, Grosch H, Schäfer J, Weltmann K D and Brandenburg R 2011 *Phys. Rev. E* **84**(4) 046404 URL <http://link.aps.org/doi/10.1103/PhysRevE.84.046404>
- [65] Becker M M, Hoder T, Brandenburg R and Loffhagen D 2013 *Journal of Physics D: Applied Physics* **46** 355203 URL <http://stacks.iop.org/0022-3727/46/i=35/a=355203>
- [66] Sigeneger F, Winkler R and Robson R E 2003 *Contributions to Plasma Physics* **43** 178–197 ISSN 1521-3986 URL <http://dx.doi.org/10.1002/ctpp.200310014>
- [67] Golubovskii Y B, Kozakov R V, Behnke J, Wilke C and Nekutchayev V O 2003 *Phys. Rev. E* **68**(2) 026404 URL <https://link.aps.org/doi/10.1103/PhysRevE.68.026404>
- [68] Dyatko N A, Ionikh Y Z, Kochetov I V, Marinov D L, Meshchanov A V, Napartovich A P, Petrov F B and Starostin S A 2008 *Journal of Physics D: Applied Physics* **41** 055204 URL <http://stacks.iop.org/0022-3727/41/i=5/a=055204>

- [69] Vrhovac S B and Petrović Z L 1996 *Phys. Rev. E* **53**(4) 4012–4025 URL <https://link.aps.org/doi/10.1103/PhysRevE.53.4012>
- [70] Petrović Z L and Phelps A V 1997 *Phys. Rev. E* **56**(5) 5920–5931 URL <https://link.aps.org/doi/10.1103/PhysRevE.56.5920>
- [71] Gallimberti I, Hepworth J K and Klewe R C 1974 *Journal of Physics D: Applied Physics* **7** 880 URL <http://stacks.iop.org/0022-3727/7/i=6/a=315>
- [72] Hoder T, Bonaventura Z, Bourdon A and Šimek M 2015 *Journal of Applied Physics* **117** 073302 URL <http://dx.doi.org/10.1063/1.4913215>
- [73] Dilecce G 2014 *Plasma Sources Science and Technology* **23** 015011 URL <http://stacks.iop.org/0963-0252/23/i=1/a=015011>
- [74] Valk F, Aints M, Paris P, Plank T, Maksimov J and Tamm A 2010 *Journal of Physics D: Applied Physics* **43** 385202 URL <http://stacks.iop.org/0022-3727/43/i=38/a=385202>
- [75] Dilecce G, Ambrico P F and Benedictis S D 2010 *Journal of Physics D: Applied Physics* **43** 195201 URL <http://stacks.iop.org/0022-3727/43/i=19/a=195201>
- [76] Paris P, Aints M, Valk F, Plank T, Haljaste A, Kozlov K V and Wagner H E 2005 *Journal of Physics D: Applied Physics* **38** 3894 URL <http://stacks.iop.org/0022-3727/38/i=21/a=010>
- [77] Pancheshnyi S 2006 *Journal of Physics D: Applied Physics* **39** 1708 URL <http://stacks.iop.org/0022-3727/39/i=8/a=N01>
- [78] Shcherbakov Y V and Sigmond R S 2007 *Journal of Physics D: Applied Physics* **40** 460 URL <http://stacks.iop.org/0022-3727/40/i=2/a=023>
- [79] Naidis G V 2009 *Phys. Rev. E* **79**(5) 057401 URL <https://link.aps.org/doi/10.1103/PhysRevE.79.057401>
- [80] Bonaventura Z, Bourdon A, Celestin S and Pasko V P 2011 *Plasma Sources Science and Technology* **20** 035012 URL <http://stacks.iop.org/0963-0252/20/i=3/a=035012>
- [81] Šimek M 2014 *Journal of Physics D: Applied Physics* **47** 463001 URL <http://stacks.iop.org/0022-3727/47/i=46/a=463001>
- [82] Černák M and Hosokawa T 1991 *Phys. Rev. A* **43**(2) 1107–1109 URL <http://link.aps.org/doi/10.1103/PhysRevA.43.1107>
- [83] Černák M, Bessières D and Paillol J 2011 *Journal of Applied Physics* **110** 053303 URL <http://dx.doi.org/10.1063/1.3630015>

- [84] Hoder T, Loffhagen D, Voráč J, Becker M M and Brandenburg R 2016 *Plasma Sources Science and Technology* **25** 025017 URL <http://stacks.iop.org/0963-0252/25/i=2/a=025017>
- [85] Celestin S, Canes-Boussard G, Guaitella O, Bourdon A and Rousseau A 2008 *Journal of Physics D: Applied Physics* **41** 205214 URL <http://stacks.iop.org/0022-3727/41/i=20/a=205214>
- [86] Stollenwerk L, Laven J G and Purwins H G 2007 *Phys. Rev. Lett.* **98**(25) 255001 URL <https://link.aps.org/doi/10.1103/PhysRevLett.98.255001>
- [87] Wild R and Stollenwerk L 2014 *New Journal of Physics* **16** 113040 URL <http://stacks.iop.org/1367-2630/16/i=11/a=113040>
- [88] Hoder T, Synek P, Chorvát D, Ráhel J, Brandenburg R and Černák M 2017 *Plasma Physics and Controlled Fusion* **59** 074001 URL <http://stacks.iop.org/0741-3335/59/i=7/a=074001>
- [89] Černák M, Hosokawa T and Odrobina I 1993 *Journal of Physics D: Applied Physics* **26** 607 URL <http://stacks.iop.org/0022-3727/26/i=4/a=013>
- [90] Pipa A V, Hoder T, Koskulics J, Schmidt M and Brandenburg R 2012 *Review of Scientific Instruments* **83** 075111 URL <http://dx.doi.org/10.1063/1.4737623>
- [91] Pipa A V, Koskulics J, Brandenburg R and Hoder T 2012 *Review of Scientific Instruments* **83** 115112 URL <http://dx.doi.org/10.1063/1.4767637>
- [92] Hoder T, Šimek M, Bonaventura Z, Prukner V and Gordillo-Vázquez F J 2016 *Plasma Sources Science and Technology* **25** 045021 URL <http://stacks.iop.org/0963-0252/25/i=4/a=045021>
- [93] Babaeva N Y, Tereshonok D V and Naidis G V 2016 *Plasma Sources Science and Technology* **25** 044008 URL <http://stacks.iop.org/0963-0252/25/i=4/a=044008>
- [94] Kulikovskiy A A 1998 *Phys. Rev. E* **57**(6) 7066–7074 URL <https://link.aps.org/doi/10.1103/PhysRevE.57.7066>
- [95] Sretenović G B, Krstić I B, Kovačević V V, Obradović B M and Kuraica M M 2014 *Journal of Physics D: Applied Physics* **47** 355201 URL <http://stacks.iop.org/0022-3727/47/i=35/a=355201>
- [96] Janda M, Hoder T, Sarani A, Brandenburg R and Machala Z 2017 *Plasma Sources Science and Technology* **26** 055010 URL <http://stacks.iop.org/0963-0252/26/i=5/a=055010>
- [97] Marode E 1975 *Journal of Applied Physics* **46** 2005–2015 (Preprint <http://dx.doi.org/10.1063/1.321882>) URL <http://dx.doi.org/10.1063/1.321882>

- [98] Korge H, Laan M and Paris P 1993 *Journal of Physics D: Applied Physics* **26** 231
URL <http://stacks.iop.org/0022-3727/26/i=2/a=010>
- [99] Jidenko N, Petit M and Borra J P 2006 *Journal of Physics D: Applied Physics* **39**
281 URL <http://stacks.iop.org/0022-3727/39/i=2/a=008>
- [100] Liu S and Neiger M 2003 *Journal of Physics D: Applied Physics* **36** 3144 URL
<http://stacks.iop.org/0022-3727/36/i=24/a=009>
- [101] Falkenstein Z and Coogan J J 1997 *Journal of Physics D: Applied Physics* **30** 817
URL <http://stacks.iop.org/0022-3727/30/i=5/a=015>
- [102] Pipa A V, Hoder T and Brandenburg R 2013 *Contributions to Plasma
Physics* **53** 469–480 ISSN 1521-3986 URL [http://dx.doi.org/10.1002/ctpp.
201200126](http://dx.doi.org/10.1002/ctpp.201200126)

Commented articles

On the next pages the original authors's work is presented as a collection of in the text commented 14 reviewed scientific articles. They are listed in following order:

1. **Hoder T**, Brandenburg R, Basner R, Weltmann K D, Kozlov K V and Wagner H E 2010 A comparative study of three different types of barrier discharges in air at atmospheric pressure by cross-correlation spectroscopy *Journal of Physics D: Applied Physics* **43** 124009
2. Grosch H, **Hoder T**, Weltmann K D and Brandenburg R 2010 Spatio-temporal development of microdischarges in a surface barrier discharge arrangement in air at atmospheric pressure *The European Physical Journal D* **60** 547–553 ISSN 1434-6079
3. **Hoder T**, Höft H, Kettlitz M, Weltmann K D and Brandenburg R 2012 Barrier discharges driven by sub-microsecond pulses at atmospheric pressure: Breakdown manipulation by pulse width *Physics of Plasmas* **19** 070701
4. Höft H, Kettlitz M, **Hoder T**, Weltmann K D and Brandenburg R 2013 The influence of O-2 content on the spatio-temporal development of pulsed driven dielectric barrier discharges in O-2/N-2 gas mixtures *Journal of Physics D: Applied Physics* **46** 095202
5. Höft H, Kettlitz M, Becker M M, **Hoder T**, Loffhagen D, Brandenburg R and Weltmann K D 2014 Breakdown characteristics in pulsed-driven dielectric barrier discharges: influence of the pre-breakdown phase due to volume memory effects *Journal of Physics D: Applied Physics* **47** 465206
6. **Hoder T**, Loffhagen D, Wilke C, Grosch H, Schäfer J, Weltmann KD and Brandenburg R 2011 Striated microdischarges in an asymmetric barrier discharge in argon at atmospheric pressure *Physical Review E* **84**(4) 046404
7. Becker M M, **Hoder T**, Brandenburg R and Loffhagen D 2013 Analysis of microdischarges in asymmetric dielectric barrier discharges in argon *Journal of Physics D: Applied Physics* **46** 355203
8. **Hoder T**, Bonaventura Z, Bourdon A and Šimek M 2015 Sub-nanosecond delays of light emitted by streamer in atmospheric pressure air: Analysis of $N_2^+(C^3\Pi_u)_{v'=0}$ and $N_2(C^3\Pi_u)_{v'=0}$ emissions and fundamental streamer structure *Journal of Applied Physics* **117** 073302

9. **Hoder T**, Černák M, Paillol J, Loffhagen D and Brandenburg R 2012 High-resolution measurements of the electric field at the streamer arrival to the cathode: A unification of the streamer-initiated gas-breakdown mechanism *Physical Review E* **86**(5) 055401
10. **Hoder T**, Loffhagen D, Voráč J, Becker M M and Brandenburg R 2016 Analysis of the electric field development and the relaxation of electron velocity distribution function for nanosecond breakdown in air *Plasma Sources Science and Technology* **25** 025017
11. **Hoder T**, Synek P, Chorvát D, Ráhel J, Brandenburg R and Černák M 2017 Complex interaction of subsequent surface streamers via deposited charge: a high-resolution experimental study *Plasma Physics and Controlled Fusion* **59** 074001
12. **Hoder T**, Šimek M, Bonaventura Z, Prukner V and Gordillo-Vázquez F J 2016 Radially and temporally resolved electric field of positive streamers in air and modelling of the induced plasma chemistry *Plasma Sources Science and Technology* **25** 045021
13. Pipa A V, **Hoder T**, Koskulics J, Schmidt M and Brandenburg R 2012 Experimental determination of dielectric barrier discharge capacitance *Review of Scientific Instruments* **83** 075111
14. Pipa A V, Koskulics J, Brandenburg R and **Hoder T** 2012 The simplest equivalent circuit of a pulsed dielectric barrier discharge and the determination of the gas gap charge transfer *Review of Scientific Instruments* **83** 115112

